Nanocavities trapped along fibrin fibers allow the diffusion of thrombolytic drugs

Marco De Spirito, Mauro Missori, Giuseppe Maulucci, Josè Teixeira, and Massimiliano Papi

Citation: Appl. Phys. Lett. **99**, 223701 (2011); doi: 10.1063/1.3657464

View online: http://dx.doi.org/10.1063/1.3657464

View Table of Contents: http://apl.aip.org/resource/1/APPLAB/v99/i22

Published by the American Institute of Physics.

Nanocavities trapped along fibrin fibers allow the diffusion of thrombolytic drugs

Marco De Spirito,[1,2,a)] Mauro Missori,[3] Giuseppe Maulucci,[1] Josè Teixeira,[4] and Massimiliano Papi[1]
[1]*Istituto di Fisica, Università Cattolica S. Cuore, L.go Francesco Vito 1, Rome I-00168, Italy*
[2]*Fondazione di Ricerca e Cura "Giovanni Paolo II" L.go A. Gemelli, 1 – Campobasso 86100, Italy*
[3]*Consiglio Nazionale delle Ricerche, Istituto dei Sistemi Complessi, Via del Fosso del Cavaliere 100, Rome 00133, Italy*
[4]*Laboratoire Lèon Brillouin (CEA/CNRS), Saclay, Gif-sur-Yvette F-91191, France*

(Received 12 July 2011; accepted 4 October 2011; published online 1 December 2011)

Ischemic heart disease consists in the formation of an occluding thrombus which hinders blood flow. The dissolution of the network of fibrin fibers, which constitute the thrombus scaffold, by using thrombolitic drugs is the most common pharmacological therapy. In this paper, by using small angle neutron scattering, we report the evidence of the presence of solvent filled cylindrical nanocavities, trapped along fibrin fibers, of diameter $R = 3.2 \pm 0.1$ nm and length $L = 22 \pm 2$ nm. The characterization of intra-fiber nanocavities furnishes a quantitative tool for the design of new enzymes which, by diffusing into fibrin fibers, fasten the thrombus lysis. © *2011 American Institute of Physics*. [doi:10.1063/1.3657464]

The fibrin gel is a three-dimensional fibrous network where platelets and other blood constituents are trapped, giving rise to the haemostatic plug (thrombus).[1–3] Pharmacological approaches to ischemic heart disease are based on the use of thrombolitic drugs which, by diffusing into the clot and inside the fibrin fibers, promote clot lysis.[2] In this context, since fibrin fibers dissolution is strongly influenced by solvent accessibility, the arrangement of solvents within the polymeric structure is extremely relevant.

The thrombin catalyzed polymerization process leads to the formation of fibrin oligomers called protofibrils that successively associate each other and form a three-dimensional network.[3–12]

With the advent of thrombolytic agents that favor the clot lysis the knowledge of the internal architecture became a crucial requirements in the design of appropriate drugs, although still poorly investigated and controversial.[3,13–15]

In this letter, we investigated the nano-scale structure of a fully hydrated gel, prepared in para-physiological condition by using small angle neutron scattering (SANS).

Gels were grown from fibrinogen solutions ($c = 30$ mg/ml) and activated with thrombin at a constant molar ratio of fibrinogen/thrombin = 100 in Tris-HCl 50 mM, EDTA-Na2 1 mM, and a *p*H 7.4 buffer with 100 mM of NaCl.[6,11,16,17] Samples were then transferred in sealed Hellma quartz cuvettes with optical path 1 mm (hydrated gels).

SANS measurements were performed on the PAXE SANS beam line at Laboratoire Lèon Brillouin (LLB), Saclay, France, with a wavevector $q = (4\pi/\lambda)\sin(\theta/2)$ ranging from 0.0632 to 1.85 nm^{-1}.[18] In Fig. 1, the typical intensity profiles of neutrons scattered by fully hydrated fibrin gels are reported (full dots). A nice shaped curve made of an initial power law decay, occurring at low q is followed by an evident shoulder at q larger than 0.1 nm^{-1}. The origin of this broad shoulder is controversial: it can arise from both (1) an highly disordered arrangement of protofibrils inside a single fiber and (2) the presence of small solvent filled cavities trapped inside fibers, as recently observed on cellulose fibers.[19–21]

To address this issue, we dried the sample in a dust-free environment to reduce, as much as possible, the presence of the solvent. Dried sample integrity has been checked by scanning the sample surface by using atomic force microscopy (SP-Magic SX (Elbatech, Italy) (see inset of Fig. 2). A continuous network of thick fibers ($\delta = 497 \pm 93$ nm) anastomosed with each other and oriented in several

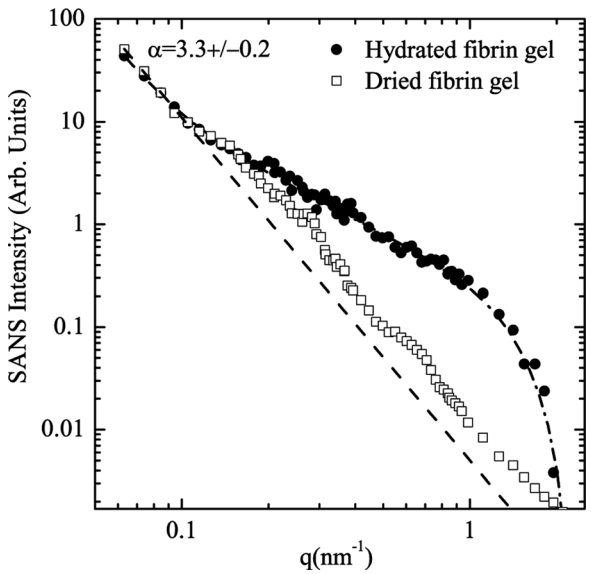

FIG. 1. Neutrons scattering intensities $I(q)$, subtracted from the incoherent background, from both hydrated (full dot) and dried fibrin (open circles) gels are reported. The evident shoulder, occurring at q larger than 0.1 nm^{-1}, in hydrated samples disappears on dried samples. The low q region of both intensity profiles are well fitted by the Porod law (dashed line). Equation (1), representing the scattering contribution arising from polymers and solvent nanocavities, perfectly fit the intensity distribution of hydrated sample (dot-dashed line).

a)Author to whom correspondence should be addressed. Electronic mail: m.despirito@rm.unicatt.it.

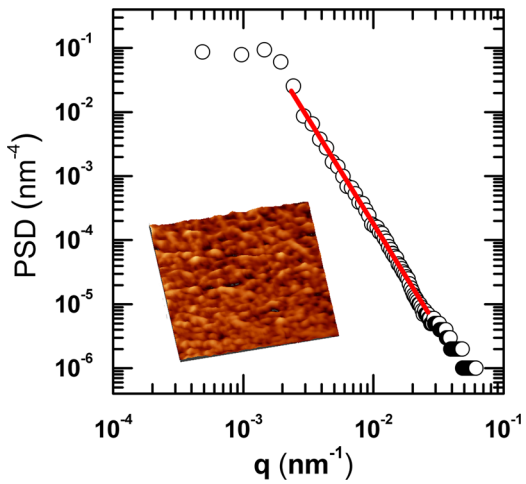

FIG. 2. (Color online) Representative AFM image ($11.5 \times 11.5\,\mu$m) of dried fibrin fibers. A continuous network of thick fibers ($\delta = 497 \pm 93$ nm) anastomosed with each other and oriented in several different directions can be observed. The power spectrum density (open circle), calculated from AFM topography, allows for the calculation of the surface fractal dimension ($D_s = 2.7 \pm 0.2$).

different directions can be observed. The fiber diameter ($\delta = 422 \pm 53$ nm) independently recovered from scanning electron microscope (SUPRA 25, Zeiss, Germany) micrographs in fully hydrated clots (Fig. 3(a)), compare well with those observed on hydrated samples.

The neutron intensity profile of a dried sample is reported in Fig. 1 (open square). The low q region, following a small intensity rescaling, well superimpose to those obtained from hydrated gel, a clear evidence that, in this low q region, the solvent contribution is negligible. In the large q region, instead, the shoulder observed in the hydrated gel almost disappears implying that solvent clusters embedded in the gel, acting as powerful scatterers, provide a not negligible coherent scattering contribution which rapidly vanishing at low q.[19,20]

To recover the size and the shape of the nano-clusters, let us imagine the inner structure of fibrin gel fibers as

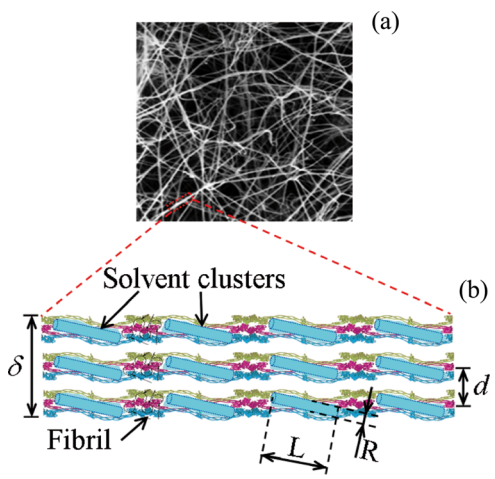

FIG. 3. (Color online) Fibrin gel supermolecular structure. In panel (a), a representative SEM micrographs ($25 \times 25\,\mu$m) of a fully hydrated gels is reported. A network of entangled fibrin fibers of diameter $\delta = 422 \pm 53$ nm is clearly visible. The inner structure of each fibrin fibers of diameter is sketched as a collection of packed protofibrils. (panel (b)). Solvent nanocavities schematized as cylindrical objects of diameter R and length L are regularly displaced within the fibers.

composed of a collection of densely packed protofibrils with vacancies (cavities), able to trap solvents locally, distributed along the axis of the fibers. The neutron scattered profile, therefore, should arises from two distinct structures: fibrin fibers, which constitute the polymer network, and solvent cavities trapped in the systematic vacancies (Fig. 3(b)). Neutron counts, recorded within a solid angle $d\Omega$ in a single detector pixel and in a time interval t, can be expressed as[22] $I(q) \sim \Delta\zeta^2\ P(q)\ S(q)$. S(q) is the structure factor and describes the spatial correlation between each scatterer's center of mass, the form factor P(q) describes the internal structure of each scatterer, and $\Delta\zeta^2$ is the square difference in neutron scattering length density (contrast).[20] The scattered intensity for the two structures can be expressed as

$$I(q) = A_1 S_1(q) P_1(q) + A_2 S_2(q) P_2(q) + B_{inc}, \qquad (1)$$

where A_1 and A_2 are constants that depend on the number density of the scatterers and on the contrast between the scatterers and the surrounding media of the two contributions (fibrin fibers and solvent cavities, respectively) and B_{inc} is a q-independent scattering contribution essentially due to the incoherent cross section of hydrogen atoms.[22] Notably in the calculation of the scattered intensity, we should account for the interactions of the waves scattered in the different phases. However, any correlation between the density fluctuations in the two phases across the phase boundaries is likely to be of short range, and consequently for small q, this contribution is small and can be neglected.[23]

Fibrin fibers are made of an assembly of oriented protofibrils with an average diameter δ (Ref. 5) (Fig. 3(b)). Since length scales probed by neutrons are much smaller than δ, the structure factor can be neglected (i.e., $S_1(q) = 1$) and the form factor reduces to the Porod law $P_1(q) \sim q^{-\alpha}$ where the exponent α is proportional to the surface fractal dimension $D_s = 6 - \alpha$.[17,19,20]

The shape of solvent cavities, in the protofibrils architecture, is supposed to posses an elongated shape (see Ref. 5 and Fig. 3(b)), and, therefore, solvent cavities have been likened to a collection of cylinders of radius R and length L. A collection of cylindrical objects, distributed in the space along a preferential direction, are characterized by a specific form ($P_2(q)$) and structure ($S_2(q)$) factor.[18,24]

The form factor for a cylinder is:[24]

$$P_2(q) = \int_0^{\pi/2} \sin\theta \left[J_0(qH\cos\theta \frac{J_1(qR\cos\theta)}{qR\sin\theta} \right]^2 d\theta, \qquad (2)$$

where $J_0(x)$ and $J_1(x)$ are the zero and first order Bessel functions, respectively, $H = L/2$ is the cylinder half-length, θ is the angle between the cylinder axis and the integral over θ averages the form factor over all the possible orientations of the cylinder with respect to q.

The spatial distribution of these cylindrical cavities, layered inside each fiber (Fig. 3(b)) depends, at the end, both on the regularity of fibrin fibers' packaging and on the bending/stretching of the surrounding polymer structure. In a first approximation, because of the huge flexibility of fibrin fibers, we do not expect an detectable contribution arising

from the short range order of water clusters and we set $S_2(q) = 1$.

The fit of Eq. (1) to SANS data from hydrated sample is reported in Fig. 2 (dash-dotted line). Equation (1) very impressively recover experimental data in all the q-range investigated with $\alpha = 3.3 \pm 0.2$, $R = 3.2 \pm 0.2$ nm, and $L = 22 \pm 2$ nm. The values of α obtained in case of dried sample ($\alpha = 3.3 \pm 0.2$), determined over the first low q points of the SANS intensity, perfectly match those obtained from hydrated samples and is a further proof of the unaltered sample integrity. The small deviation in the dry sample of SANS data from the power law decay (Fig. 1, open squares) at large q should still account for the internal structure of fibrin fibers.

The value of α, in the case of dried sample, can also be, independently, recovered from the power spectrum density (PSD) calculated from AFM topography[20] (Fig. 2). Indeed, for self similar surfaces, the fractal surface dimension D_s, which characterize the PSD decays with q ($PSD \sim q^{8-2D_s}$), is related to α ($\alpha = 6\text{-}D_s$).

AFM data, therefore, allow to recover, over a q range of two decades, the value of α that, in our case ($\alpha = 3.3 \pm 0.2$), well match those obtained independently by SANS.

In throbolytic therapy, the intrinsic fibers permeability to macromolecular drugs became a relevant issue. In fact, the ready diffusional access from without to proteases involved in fibrinolysis is not obvious.[25] In this context, we demonstrated the possibility of monitoring the access of solvent to fibers, by analyzing SANS data without any solvent exchange (i.e., deuterium) to enhance the scattering contrast.

The accessibility of solvents and external agents to fiber through nano-cavities distributed along fibrin fibers gives a quantitative foundation to all of those pharmaceuticals therapy were small enzymes, able to penetrate inside cloth's fibers, are employed to fasten the cloth lysis.

Some of the experimental data reported in this paper were obtained at the LABCEMI (Laboratorio Centralizzato di Microscopia, Ottica ed Elettronica) of the Università Cattolica del S. Cuore di Roma (Italy). This research was supported by the Università Cattolica del Sacro Cuore, Roma, Italy.

[1]R. F. Doolittle, Annu. Rev. Biochem. **53**, 195 (1984).
[2]B. Blombäck, K. Carlsson, K. Fatah, B. Hessel, and R. Procyk, Thromb. Res. **75**, 521 (1994).
[3]G. Caracciolo, M. De Spirito, A. C. Castellano, D. Pozzi, G. Amiconi, A. De Pascalis, R. Caminiti, and G. Arcovito, Thromb. Haemost. **89**, 632 (2003).
[4]D. V. Sakharov, J. F. Nagelkerkel, and D. C. Rijken, J. Biol. Chem. **271**, 2133 (1996).
[5]Z. Yang, I. Mochalkin, and R. F. Doolitle, Proc. Natl. Acad. Sci. U.S.A. **97**, 14156 (2000).
[6]F. Ferri, M. Greco, G. Arcovito, F. A. Bassi, M. De Spirito, E. Paganini, and M. Rocco, Phys. Rev. E **63**, 0314011 (2001).
[7]F. Ferri, M. Greco, G. Arcovito, M. De Spirito, and M. Rocco, Phys. Rev. E **66**, 0119131 (2002).
[8]M. W. Mosesson, J. Thromb. Haemostasis **8**, 1894 (2005).
[9]E. Di Cera, Q. D. Dang, and Y. M. Ayala, Cell. Mol. Life Sci. **53**, 701 (1997).
[10]E. Di Stasio, C. Nagaswami, J. W. Weisel, and E. Di Cera, Biophys. J. **75**, 1973 (1998).
[11]M. Papi, G. Arcovito, M. De Spirito, G. Amiconi, A. Bellelli, and G. Boumis, Appl. Phys. Lett. **86**, 183901 (2005).
[12]M. De Spirito, G. Arcòvito, M. Papi, M. Rocco, and F. Ferri, J. Appl. Cryst. **36**, 636 (2003).
[13]S. L. Diamond, Annu. Rev. Biomed. Eng. **1**, 427 (1999).
[14]J. Torbet, J. M. Freyssent, and G. H. Hudry-Clergeon, Nature **289**, 1189 (1981).
[15]K. M. Weigandt, C. Danilo, D. C. Pozzo, and L. Porcar, Soft Matter **5**, 4321 (2009).
[16]R. De Cristofaro and E. Di Cera, J. Mol. Biol. **226**, 1077 (1980).
[17]M. Missori, M. Papi, G. Maulucci, G. Arcovito, G. Boumis, A. Bellelli, G. Amiconi, and M. De Spirito, Eur. Biophys. J. **39**, 1001 (2010).
[18]S. H. Chen, J. S. Huang, and P. Tartaglia, *Structure and Dynamics of Strongly Interacting Colloids and Supra-molecular Aggregates in Solution* (Kluwer Academic Publishers, Dordrecht, 1992).
[19]M. Missori, C. Mondelli, M. De Spirito, C. Castellano, M. Bicchieri, R. Schweins, G. Arcovito, M. Papi, and A. C. Castellano, Phys. Rev. Lett. **97**, 238001 (2006).
[20]M. De Spirito, M. Missori, M. Papi, G. Maulucci, J. Teixeira, C. Castellano, and G. Arcovito, Phys. Rev. E **77**, 041801 (2008).
[21]M. S. Kent, G. Cheng, J. K. Murton, E. L. Carles, D. C. Dibble, F. Zendejas, M. A. Rodriquez, H. Tran, B. Holmes, B. A. Simmons, B. Knierim, M. Auer, J. L. Banuelos, J. Urquidi, and R. P. Hjelm, Biomacromolecules **11**, 357 (2010).
[22]R. J. Roe, *Methods of X-ray and Neutron Scattering in Polymer Science* (Oxford University Press, New York, 2000).
[23]A. Guinier and G. Fournet, *Small-Angle Scattering of X-rays* (Wiley, New York, 1955).
[24]M. Kerker, *The Scattering of Light and Other Electromagnetic Radiation* (Academic, New York, 1969).
[25]P. A. McKee, P. Mattock, and R. L. Hill, Proc. Natl. Acad. Sci. U.S.A. **66**, 738 (1970).